A STUDY ON THE SYNTHESIS OF MoS_2/rGO AND THE INVESTIGATION OF THEIR CHARGE-DISCHARGE PROPERTIES WHEN USED AS CATHODE MATERIAL IN A RECHARGEABLE Zn-ion BATTERY

Kien Nguyen-Ba[1*], Huy Le-Quoc[1], Anh T. Vo[1], Khan Dinh-Thanh[2], Duc Binh Luu[1*]

[1]*The University of Danang - University of Science and Technology*
[2]*The University of Danang - University of Science and Education*

*Corresponding author: ldbinh@dut.udn.vn; nbkien@dut.udn.vn

(Received: April 25, 2022; Accepted: June 16, 2022)

Abstract - Recently, rechargeable aqueous Zn-ion batteries have attracted much attention and are potential candidates for grid storage applications because of their low cost and safety. However, to approach practical applications, suitable cathode materials must be developed. As a two-dimensional layered material, MoS_2-based materials are very potential candidates. Herein, MoS_2/rGO materials were synthesized by hydrothermal method and then the charge-discharge properties of the fabricated materials were investigated when they are used as cathode materials for rechargeable Zn-ion batteries. The MoS_2/rGO has an expanded interlayer, which achieves a high initial capacity of about 170 mAh/g but does not have a high stability. In contrast, the MoS_2-KOA has a low capacity but is very stable, even after 200 charge/discharge cycles. This study has shown the advantages and disadvantages of MoS_2-based materials with expanded interlayer and suggests further work to find methods to stabilize the expanded interlayer to increase the charge/discharge stability.

Key words - MoS_2/rGO material; Rechargable Zn-ion batteries; Charge/discharge; Capacity

1. Introduction

Grid energy storage technologies play a very important role in the efficient utilization of intermittent renewable - energy sources, such as solar energy and wind energy [1-3]. For many years, rechargeable lithium-ion battery technology has been used in mobile electronic devices, military, and electric vehicles because of its characteristics of lightweight, high-energy density, and high stability [4-6]. However, because of the flammability of organic-based electrolytes, the scarcity and high cost of materials used to manufacture them, and environmental concerns, the use of Li-ion batteries for grid storage applications is limited [1, 7]. To overcome these limitations, aqueous Zn-ion batteries are one of the most potential candidates because of the high theoretical specific capacity of zinc metal (820 mAh/g), low redox potential (0.76 V vs. Standard hydrogen electrode) and highly reversible in water-based electrolytes [8-9]. Combined with the advantages of Zn, such as low toxicity, abundant supply, low cost, and stability in water and air, aqueous Zn ion batteries may be widely used in the future for large capacity and stationary grid energy storage [9-10]. However, the practical application of rechargeable Zn-ion batteries is still limited by the real capacity and low charge-discharge stability resulting from the difficult diffusion and intercalation kinetics of Zn^{2+} ions in cathode materials, dissolution of cathode materials in water-based electrolytes, dendrite growth and side reactions such as hydrogen evolution reaction, corrosion on Zn metal anodes [10]. Therefore, the development of cathode materials for Zn-ion batteries is one of the biggest challenges on the way to their practical application for grid storage in the future.

To date, materials with tunneling or layered structure, including those based on manganese, vanadium, and molybdenum, have been produced and used as cathode materials for rechargeable Zn-ion batteries [11-12]. Recently, two-dimensional transition metal dichalcogenides (TMDs) with layered structure such as molybdenum disulfide (MoS_2), which are among the most studied anode materials for Li^+/Na^+ batteries [13-14], have been proven as effective cathode materials for rechargeable Zn-ion batteries [15]. It has been shown that increasing interlayer spacing and defect engineering decreases the intercalation and diffusion energies of Zn ions [16]. Normally, MoS_2 materials exist in the semiconductor 2H-MoS_2 phase, a thermodynamically stable phase but with low conductivity. To increase the electrical conductivity, MoS_2 materials are often combined with conductive substrates, such as rGO, CNTs or synthesized in the metallic 1T-phase [16]. In this study, we synthesized MoS_2-based materials with extended or non-extended interlayer spacing and investigated the charge-discharge properties of these materials when applied as cathode in Zn-ion batteries (Figure 1). We found that the extended interlayer structure increases the capacity of the battery, but the stability is not high.

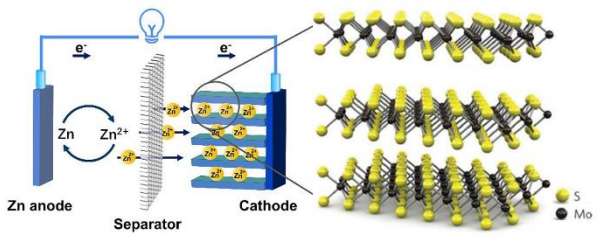

Figure 1. *Illustration of Zn-ion rechargeable batteries [17-18]*

2. Experimental section

2.1. Materials synthesis

The MoS_2/rGO material was synthesized by the hydrothermal method. First, 30 mg of graphene oxide (GO) was ultrasonically dispersed in 50 ml of double distilled water for 30 minutes, then 1000 mg of oxalic acid $(COOH)_2.2H_2O$, 450 mg of molybdenum precursor $(NH_4)_6Mo_7O_{24}.4H_2O$ and 646.7 mg of sulfur precursor

$(NH_2)_2CS$ were added and sonicated for another 30 minutes. Subsequently, the hydrothermal reaction was carried out in a Teflon-lined 100-mL stainless steel autoclave at 190ºC for 24 h. The autoclave was then removed and allowed to cool naturally. The resulting product was filtered with Whatman filter paper, washed several times with distilled water and absolute ethanol, and dried for 12 h at 60°C. The MoS_2 material was prepared by the same method but without the addition of graphene oxide. For comparison, the MoS_2 material without an addition of graphene oxide and oxalic acid was synthesized by the same method but with a synthesis temperature of 210ºC and referred to as MoS_2- KOA. The process of material synthesis is described in Figure 2.

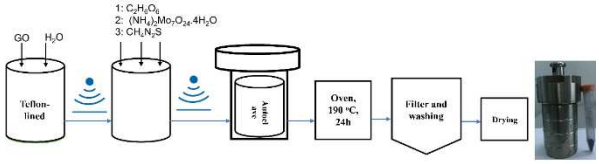

Figure 2. *Materials synthesis process*

2.2. Materials characterization

The crystal structure of the materials was determined by X-ray diffraction (XRD, D8 Bruker advanced, Germany). The morphology of the materials was analyzed by scanning electron microscope (SEM, JSM-IT200, JEOL, Japan). The elemental composition was determined by X-ray energy dispersion spectroscopy (EDS). The characteristic vibrational modes of the materials were determined using the Raman system (LabRaman, Horiba Scientific).

2.3. Measurement of charge-discharge characteristics

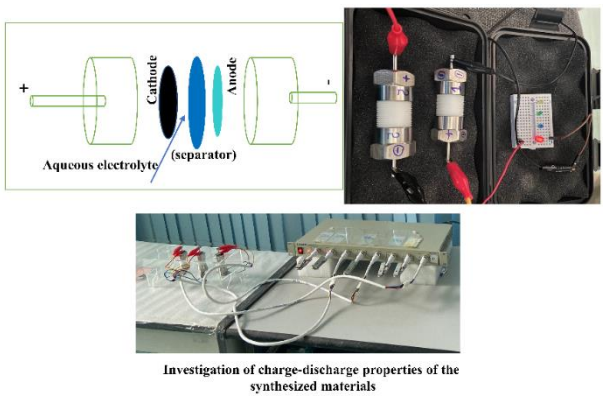

Figure 3. *Investigation of battery charge-discharge characteristics using Swagelok cells*

To prepare the cathode electrodes, the synthesized material was mixed with acetylene black (Super-P) and polyvinylidene fluoride (PVDF) in a mass ratio of 8:1:1. Then a certain amount of N-methyl-2-pyrrolidone (NMP) was added to the above mixture and ground for a certain time until a homogeneous paste was obtained. Then, the mixed material was cast evenly onto a stainless-steel foil and dried in a vacuum oven at 80°C for 8 hours. Finally, the stainless-steel foil was cut into cathode electrodes with a diameter of 10 mm and an active material mass loading of about 1.5-2.5 mg/cm^2. Zinc foil (99.9%) were was used directly as anodes with no surface treatment or modification. The glass fiber membrane with a diameter of 12 mm was used as a separator. A 3M water-based solution $(CF_3SO_3)_2Zn$ was used as the electrolyte. The Swagelok cell was built to investigate the charge-discharge characteristics with LAND battery testing system (Figure 3).

3. Results and discussion

3.1. Structural and morphology results

The crystal structure of the prepared materials was determined using the X-ray diffraction method. In Figure 4a, the XRD spectrum of the materials shows the appearance of three peaks with values of about 33.3º, 39.7º, and 57.9º, assigning to crystal planes (100), (103), and (110), respectively. These peaks are matched well with the hexagonal structure of the stable phase 2H-MoS_2 (JCPDS 73-1508) [18-19]. Furthermore, the peak corresponding to the crystal plane (002) of the MoS_2/rGO and MoS_2 materials shifts to lower-angle region of about ~10º, demonstrating that the interlayer spacing of MoS_2 is expanded from 6.15 to about 8.9 Å along the c-axis (calculated using Bragg equation: $2d\sin\theta=\lambda$) [19]. In contrast, the peak corresponding to the (002) crystal plane had a value of ~14.8º when oxalic acid was not added to the initial precursor solution, i.e., the interlayer spacing of MoS_2-KOA was not expanded [15]. The expanded interlayer spacing of MoS_2 can facilitate the intercalation of Zn^{2+} ions, leading to an increase in the capacity of the Zn-ion battery [15,19]. The MoS_2/rGO and MoS_2 materials exhibit peaks with lower and broadened intensity, showing that the synthesized materials have low crystallinity or small particle size [19]. In the absence of oxalic acid, the MoS_2-KOA material exhibits higher intensity and a narrower peak in the (002) plane than the other two materials, demonstrating its better crystallinity and larger particle size, as shown in Figure 4a. During the hydrothermal reaction, the nuclei of MoS_2 materials form and grow on GO layers, and GO is reduced to rGO (reduced graphene oxide) with better electrical conductivity. From Figure 4a, the characteristic diffraction peak at about 26º of rGO does not appear, showing that the MoS_2 has dispersed and covered the rGO layers. As seen in Figure 4b, the Raman spectra of MoS_2/rGO clearly shows the typical peaks of the 2H-MoS_2 phase at about 372.3 and 404.3 cm^{-1}, corresponding to the E12g phonon mode (in-plane vibrational mode) and A1g (out-of-plane vibrational mode), respectively [20], while the other two peaks at about 1352 cm^{-1} and 1586 cm^{-1} correspond to the characteristic bands D and G of rGO [21]. Additionally, a weaker peak can be seen at about 815 cm^{-1}, showing a small amount of MoO_3 in the hybrid MoS_2/rGO material [21]. According to Figure 4c, the Raman spectra of the MoS_2 and MoS_2-KOA materials also show peaks corresponding to the E^1_{2g} and A_{1g} phonon modes of 2H-MoS_2 [20].

The morphology of MoS_2/rGO, MoS_2 and MoS_2-KOA was studied by a scanning electron microscopy (SEM). As shown in Figures 5b, c, the SEM images of MoS_2 and MoS_2-KOA show the morphology of agglomerated flower-like particles. The size of the flower-like particles is larger when oxalic acid is not added. In contrast, the MoS_2

particles were more dispersed across the layers or clusters of rGO layers with the addition of GO in the hydrothermal reaction, as shown in Figure 5a. In addition, elemental mapping analysis (EDS) clearly confirms the presence and uniform distribution of Mo and S elements, as shown in Figure 5.

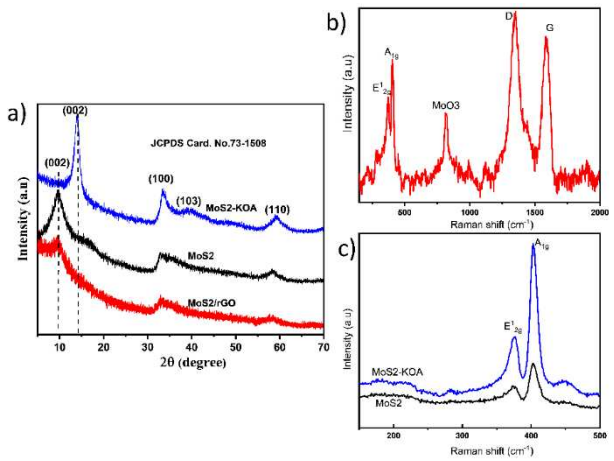

Figure 4. *XRD patterns of all 3 synthesized materials a); Raman spectra of MoS2/rGO b); Raman spectra of MoS2 and MoS2-KOA c)*

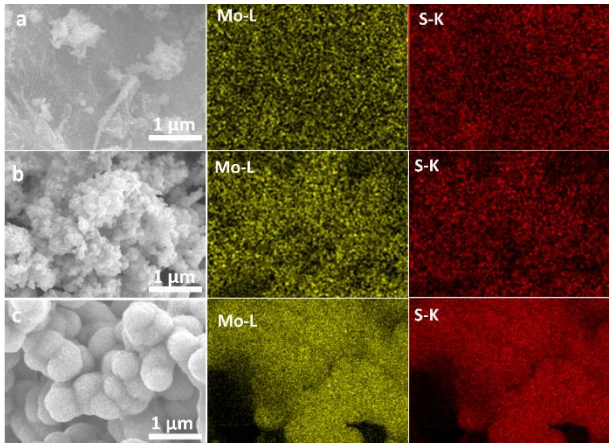

Figure 5. *SEM images and elemental mapping of MoS_2/rGO-15 a); MoS_2 b) and MoS_2-KOA c)*

3.2. Investigation of charge-discharge properties of the synthesized materials

A Swagelok battery cell was built to investigate the charge-discharge properties of the synthesized materials as cathode materials for rechargeable Zn-ion batteries with water-based electrolytes. Figure 6a shows the charge-discharge profiles of MoS_2/rGO, MoS_2 and MoS_2-KOA at 100 mA/g in a potential window of 0.25-1.3 V (against Zn^{2+}/Zn). It can be clearly seen that the MoS_2/rGO has the highest specific capacity, with a value of ~170 mAh/g, followed by the MoS_2 with a value of ~120 mAh/g. The MoS_2-KOA shows the lowest specific capacity of 20 mAh/g. This can be explained by the fact that the MoS2/rGO and MoS_2 materials have an expanded interlayer spacing that facilitates the intercalation of Zn^{2+} ions, as analyzed in the above X-ray diffraction results. In addition, the coupling of MoS_2 layers with rGO layers can increase the electrical conductivity of the MoS_2/rGO material, which increases its initial specific capacity.

Figure 6b shows the rate performance from 0.1 to 1.0 A/g of the synthesized materials. The discharge specific capacity of the MoS_2/rGO materials gradually decreases with increasing discharge rate, and when recharged at 0.1 A/g, the specific capacity of the material does not reach its original value. This could be because of the instability of the material structure with the expanded interlayer spacing and that the physical bonding between the MoS_2 and rGO layers is not uniform and strong, resulting in a decreased specific capacity during charge/discharge process [22]. For the MoS_2, it is observed that the charge-discharge performance at different rates is much better than that of MoS_2/rGO. The MoS_2-KOA material does not have an expanded interlayer spacing, although it has a low specific capacity, the charge-discharge performance at different rates is very good. In addition, the cycling stability of the materials is evaluated at the charge-discharge rate 0.1 A/g. As shown in Figure 6c, the specific capacity of the MoS_2/rGO decreases after charging and discharging at different rates, and the charge-discharge process is interrupted at the 0.1 A/g during the cycling stability test. This could be because of the collapsed expanded structure, the poor bonding between MoS_2 and the conductive rGO substrate, and the large specific capacitance that triggers the dendrite growth on the Zn anode and causes the short circuit. This speculation is appropriate because the same phenomenon occurs with the MoS2 material. Further detailed ex-situ study of the cathode after charge-discharge cycling would help to determine more clearly the reason. In contrast, the MoS_2-KOA material has a much lower specific capacity, but its stability is very high even after 200 charge and discharge cycles.

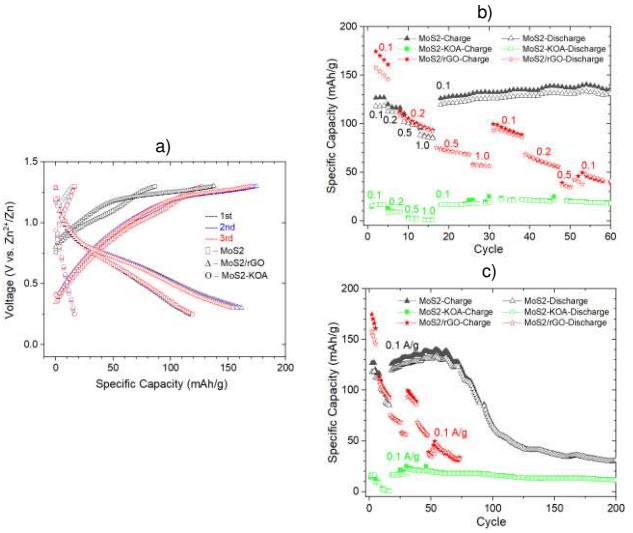

Figure 6. *Galvanostastic charge-discharge profiles at 0,1 A/g: Rate performance a); and Cycling stability at 0,1 A/g b); of MoS_2/rGO, MoS_2 and MoS_2-KOA c)*

4. Conclusions

In summary, we have successfully synthesized MoS_2-based materials by the hydrothermal method and investigated the charge-discharge properties of these materials when applied as cathode materials for Zn-ion rechargeable batteries. The MoS_2/rGO material with an

expanded interlayer structure has an initial charge-discharge specific capacity of ~170 mAh/g at 0.1 A/g rate but does not have high stability. In the absence of a conductive rGO substrate, the MoS_2 with similar expanded interlayer structure shows lower specific capacity but higher stability. However, the capacity is still reduced after about 70 cycles during the cycling stability test. In contrast, the MoS_2-KOA does not have an expanded interlayer structure, even the charge-discharge specific capacity is low, the stability is very high, even after 200 cycles. The above analyses show that the expanded interlayer structure could probably increase the capacity of the materials but is much less stable. Moreover, it is also possible that the connection and junction between the conductive substrate rGO and MoS_2 are not good. This finding will help us in the future to design a suitable synthesis strategy for MoS_2-based material that has an expanded interlayer structure but at the same time a high stability.

Acknowledgement: This research is funded by the Murata Foundation under the project code: T2021-02-01MSF.

REFERENCES

[1] Blanc, Lauren E., et al. "Scientific Challenges for the Implementation of Zn-Ion Batteries", *Joule*, vol. 4, no. 4, Elsevier Inc., 2020, pp. 771–99.

[2] Wu, Mingjie, et al. "Aqueous Zn-based Rechargeable Batteries: Recent Progress and Future Perspectives", *InfoMat*, Vol. 4, Issue 5, 2022, e12265.

[3] Du, Wencheng, et al. "Challenges in the Material and Structural Design of Zinc Anode towards High-Performance Aqueous Zinc-Ion Batteries", *Energy and Environmental Science*, vol. 13, no. 10, Royal Society of Chemistry, 2020, pp. 3330–60.

[4] Larcher, D., and J. M. Tarascon. "Towards Greener and More Sustainable Batteries for Electrical Energy Storage", *Nature Chemistry*, vol. 7, no. 1, 2015, pp. 19–29.

[5] Nitta, Naoki, et al. "Li-Ion Battery Materials: Present and Future", Materials Today, vol. 18, no. 5, Elsevier Ltd., 2015, pp. 252–64.

[6] Tian, Yaosen, et al. "*Promises and Challenges of Next-Generation 'Beyond Li-Ion' Batteries for Electric Vehicles and Grid Decarbonization*", Chemical Reviews, 2020.

[7] Nitta, Naoki, et al. "Li-Ion Battery Materials: Present and Future", *Materials Today*, vol. 18, no. 5, Elsevier Ltd., 2015, pp. 252–64.

[8] He, Pingge, and Shaowei Chen. "Cathode Strategies to Improve the Performance of Zinc-ion Batteries", *Electrochemical Science Advances*, Vol. 2, Issue 3, 2022, pp. 1–24.

[9] Yang, Qi, et al. "*Cathode Engineering for High Energy Density Aqueous Zn Batteries*", Accounts of Materials Research, 2021.

[10] Zhang, Qi, et al. "Issues and Rational Design of Aqueous Electrolyte for Zn-ion Batteries", *SusMat,* vol. 1, no. 3, 2021, pp. 432–47.

[11] Kumankuma-Sarpong, James, et al. "Advances of Metal Oxide Composite Cathodes for Aqueous Zinc-Ion Batteries", *Advanced Energy and Sustainability Research*, vol. 3, Issue 6, 2022, pp. 1-29.

[12] Yang, Qi, et al. "Cathode Engineering for High Energy Density Aqueous Zn Batteries", *Accounts of Materials Research,* vol. 3, no. 1, 2022, pp. 78–88.

[13] Wang, Ruxing, et al. "MoS_2@rGO Nanoflakes as High Performance Anode Materials in Sodium Ion Batteries", *Scientific Reports*, vol. 7, no. 1, Springer US, 2017, pp. 1–9.

[14] Zhao, Xuewen, et al. "Low Crystalline MoS_2 Nanotubes from MoS2Nanomasks for Lithium Ion Battery Applications", *ACS Applied Nano Materials,* vol. 3, no. 8, 2020, pp. 7580–7586.

[15] Liang, Hanfeng, et al. "Aqueous Zinc-Ion Storage in MoS_2 by Tuning the Intercalation Energy", *Nano Letters*, vol. 19, no. 5, 2019, pp. 3199–206.

[16] Lee, Wee Siang Vincent, et al. "Unraveling MoS_2 and Transition Metal Dichalcogenides as Functional Zinc-Ion Battery Cathode: A Perspective", *Small Methods*, vol. 5, no. 1, 2021, pp. 1–14.

[17] He, Zuoli, and Wenxiu Que. "Molybdenum Disulfide Nanomaterials: Structures, Properties, Synthesis and Recent Progress on Hydrogen Evolution Reaction", *Applied Materials Today*, vol. 3, Elsevier, June 2016, pp. 23–56.

[18] Liu, Jiapeng, et al. "Boosting Aqueous Zinc-Ion Storage in MoS_2 via Controllable Phase*", Chemical Engineering Journal,* vol. 389, 2020, pp. 1-9.

[19] Jia, Hao, et al. "Interlayer-Expanded MoS_2 Hybrid Nanospheres with Superior Zinc Storage Behavior", *Composites Communications,* vol. 27, 2021, pp. 1-5.

[20] Huang, Meihong, et al. "Hierarchical MoS2@CNTs Hybrid as a Long-Life and High-Rate Cathode for Aqueous Rechargeable Zn-Ion Batteries", *ChemElectroChem*, vol. 7, no. 20, 2020, pp. 4218–23.

[21] Muthukumar, Kamalambika, et al. "Tuning the Defects in MoS2/Reduced Graphene Oxide 2D Hybrid Materials for Optimizing Battery Performance", *Sustainable Energy and Fuels*, vol. 5, no. 16, Royal Society of Chemistry, 2021, pp. 4002–14.

[22] Liu, Huanyan, et al. "Boosting Zinc-Ion Intercalation in Hydrated MoS2 Nanosheets toward Substantially Improved Performance", *Energy Storage Materials*, vol. 35, no. November 2020, Elsevier B.V., 2021, pp. 731–38.